The relationship between thermocline depth and SST anomalies in the eastern equatorial Pacific: Seasonality and Decadal Variations

Jieshun Zhu[1,2], ***Arun Kumar***[1] *and* ***Bohua Huang***[3,4]

[1] Climate Prediction Center, NOAA/NWS/NCEP, College Park, Maryland, USA
[2] Innovim, Greenbelt, Maryland, USA
[3]Department of Atmospheric, Oceanic, and Earth Sciences, College of Science, George Mason University, Fairfax, Virginia, USA
[4]Center for Ocean-Land-Atmosphere Studies, George Mason University, Fairfax, Virginia, USA

1. Motivations

Background

A) The vital role of thermocline fluctuations in ENSO cycle was *well established*

•"Thermocline feedback" stressed in most ENSO theories (e.g., Battisti and Hirst, 1989; Suarez and Schopf, 1988; Jin, 1997);

•In simplified ENSO models (e.g., Zebiak and Cane 1997; Zhang et al. 2003), the model **thermocline** fluctuations are **parametrized** in the temperature of subsurface water entrained into the mixed layer (***Te***) which affects **SST** evolution directly.

B) The relationship between thermocline and SST in the equatorial Pacific is *not straightforward*

•By investigating their **simultaneous** relationship, Harrison and Vecchi (2001) found that significant correlations only existed in the eastern and east-central Pacific. *They concluded that it was "inappropriate to attribute SST changes to thermocline depth changes."*

•Zelle et al. (2004) explored the phase dependence of the local relationship between them and identified a **strong time-lagged relationship** (e.g. Fig.1a).

Questions to be addressed

1)The **seasonality** of the thermocline-SST relationship ??

2)The **low-frequency** variation of the relationship ??

2. Data

A) Z20 (a proxy for thermocline):

- BMRC Z20 analysis which combined data from moored buoys, expendable bathythermographs, and Argo floats (Smith, 1995): Jan. 1980 - Jul. 2012
- Z20 derived from three ocean reanalyses: ORA-S3 (Balmaseda et al. 2008; 1959-2009), ORA-S4 (Balmaseda et al. 2013; 1958-2013), and SODA (Carton and Giese 2008; 1958-2008)

B) SST:

- OISST, version 2 (Reynolds et al. 2002): late 1981 - present
- ERSST, version 3 (Smith et al., 2008): 1854 - present

C) Surface wind stress:

- ERA-Interim reanalysis (Dee et al. 2011): 1979 - present
- NCEP/NCAR reanalysis 1 (Kalnay et al. 1996): 1948 - present

3. Seasonality of Z20-SST relationship

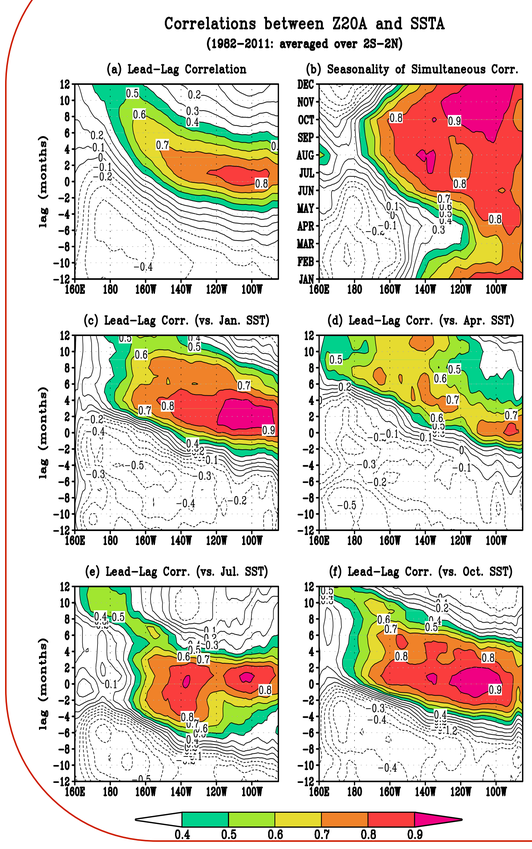

1) **Fig. 1a**: the same finding as Zelle et al. (2004) based on 1990-1999 data (a **time-lagged** Z20-SST relationship; the longer lag appears when moving westwards);

2) **Figs. 1c-f**: lead-lag relationship exhibits a strong **seasonal** variation (weaker in spring);

3) **Fig. 1b**: Simultaneous correlation (weakest during spring and strongest during the late autumn and winter)

Fig. 1 Lead-lag correlations between observed Z20 and SST anomalies for (a) all months regardless of season, (c) January, (d) April, (e) July, and (f) October. (b) Simultaneous correlations between observed Z20 and SST anomalies as a function of season. Positive lag means Z20 leads SST. All calculations are based on 1982–2011 and presented along the equator (averaged over 2ºS–2ºN).

4. Verification with SST_nudged CGCM simulations

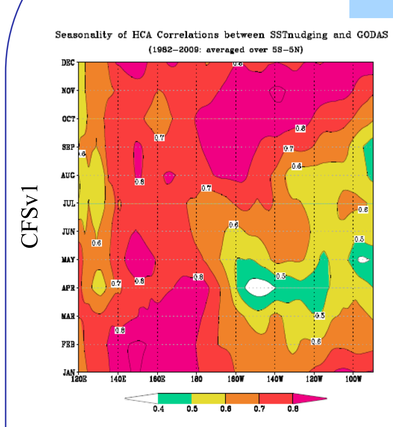

Experiments description

Running coupled models with model SSTs strongly nudged to observations:

1) CFSv1: 9-members; 1982-2009 (Wang et al. 2013; Kumar et al. 2014)

2) CFSv2L: 6-members; 1982-2010

Fig. 2a Seasonality (monthly variation) of anomaly correlations between GODAS analyzed heat-content anomalies and those derived by **CFSv1** with SSTs nudged to observations along the equator (averaged over 5ºS–5ºN) in the Pacific. (copied from Zhu et al. 2015 *Mon. Wea. Rev.*)

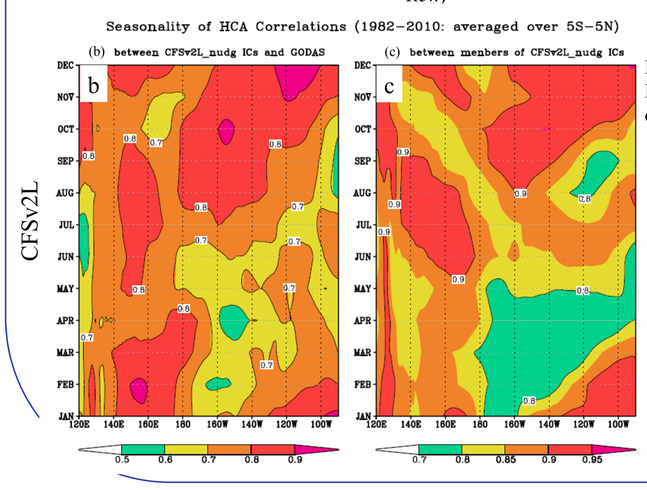

Fig. 2b Same as in Fig. 5a, but for **CFSv2L** simulations
Fig. 2c Same as in Fig. 5b, but the correlation between members of **CFSv2L** simulations

1) **Fig. 2a,b**: Both models derived subsurface conditions the **least accurately in spring**, even though CFSv2L is better than CFSv1;

2) **Figs. 2c:** Ensemble members are the **least consistent in spring** for CFSv2L.

5. Linkage with ENSO spring barrier and **Decadal** variations

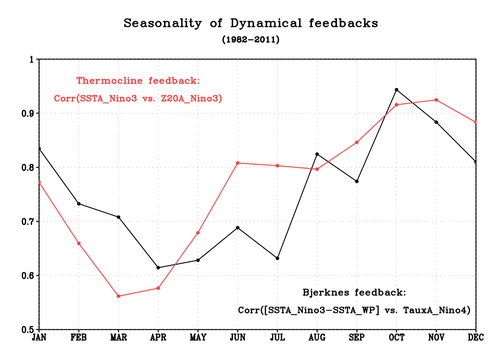

***Background**: The upper ocean heat content variations (or **D20** fluctuation) present **strongest persistence in spring**, which prompted a argument that initialization of OHC may "overcome" the spring barrier in SST prediction skill (McPhaden, 2003).*

However, the D20-SST linkage is **weakest in spring**, as the Bjerknes feedback (Fig. 3), both of which could contribute to the ENSO spring persistence barrier.

Fig. 3 Simultaneous correlations as a function of season between the observed Z20 and SST anomalies averaged over the Niño3 region (red curve) and between the observed SST zonal gradients and the surface zonal wind stress anomalies averaged over the Niño 4 region (black curve). The SST zonal gradient is defined as the difference between the western Pacific region (120ºE–160ºE, 5ºS–5ºN) and the Niño 3 region. Calculations are performed for 1982–2011.

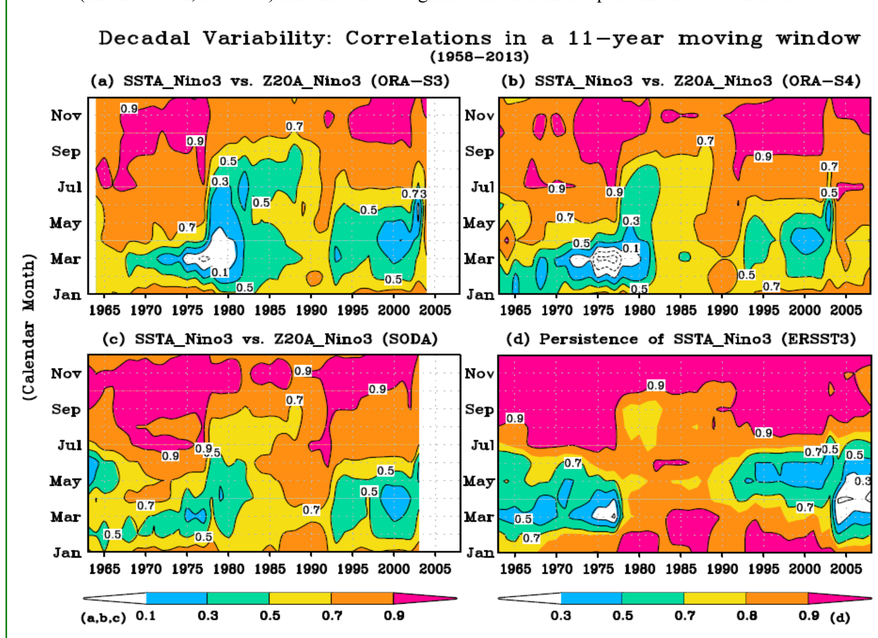

Fig. 4 Simultaneous correlations between Z20 and SST anomalies averaged over the Niño3 region as a function of season within an 11 year moving window, with SST data from ERSST3 and Z20 data from (a) ORA-S3, (b) ORA-S4, and (c) SODA. (d) Seasonality of Niño3 SST anomalies persistence within an 11 year moving window. The persistence for a given month (e.g., March) is defined as the correlation between two time series for 1month earlier (February) and later (April) than the month. The 11 year window is shifted year by year from 1958 to 2013.

1) **Fig. 4d**: Decadal variations of ENSO persistence barrier (*absent during the whole 1980s and the early 1990s, and the timing changes*);

2) **Figs. 4a-c**: The Z20-SST relationship also exhibits low-frequency variations, which correspond well to the decadal variations of ENSO persistence barrier [*the weakest correlation tends to appear in March before 1980s, while it occurs at least 1month late (i.e., in April) during 1993–2003*];

3) **Fig. 5**: Two factors might contribute to the difference in timing of low D20-SST correlations between 1965-1980 and 1993-2003 – the time shift in the seasonal cycles of ***Taux*** (Fig. 5a vs. Fig. 5b) and ***Z20*** (Fig. 5c vs. Fig. 5d).

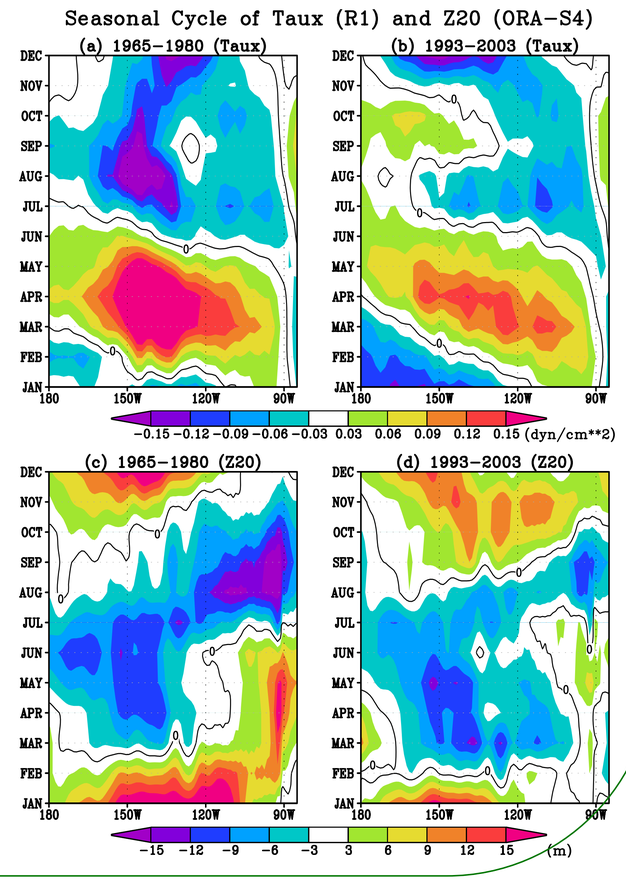

Fig. 5 Seasonal cycle of surface zonal wind stress (dyn/cm**2) and Z20 (m) along the equator (averaged over 2ºS–2ºN) with the annual mean climatology removed, based on the periods of (a and c) 1965–1980 and (b and d) 1993–2003.

6. Key Points

1) Strong seasonality is found in the Z20 and SST relationship: weakest during spring;

2) The seasonality could be seen in CGCM simulations with model SSTs strongly nudged to observations;

3) Decadal shift of Z20-SST relationship agrees with ENSO SST persistence changes.

7. References

Harrison, D., and G. A. Vecchi (2001), El Niño and La Niña-Equatorial Pacific thermocline depth and sea surface temperature anomalies, 1986–98, *Geophys. Res. Lett.*, **28**, 1051–1054, doi:10.1029/1999GL011307.

Kumar, A., H.Wang, Y. Xue, and W. Wang, 2014: Howmuch ofmonthly subsurface temperature variability in the equatorial Pacific can be recovered by the specification of sea surface temperatures? *J. Climate*, **27**, 1559–1577.

McPhaden, M. J. (2003), Tropical Pacific Ocean heat content variations and ENSO persistence barriers, *Geophys. Res. Lett.*, **30**(9), 1480, doi:10.1029/2003GL016872.

Zelle, H., G. Appeldoorn, G. Burgers, and G. J. van Oldenborgh (2004), The relationship between sea surface temperature and thermocline depth in the eastern equatorial Pacific, *J. Phys. Oceanogr.*, **34**, 643–655, doi:10.1175/2523.1.

Zhu, J., A. Kumar, H. Wang and B. Huang (2015) Sea Surface Temperature Predictions in NCEP CFSv2 Using a Simple Ocean Initialization Scheme. *Mon. Wea. Rev.*, **143**, 3176–3191.

Zhu, J., A. Kumar, and B. Huang (2015), The relationship between thermocline depth and SST anomalies in the eastern equatorial Pacific: Seasonality and decadal variations, *Geophys. Res. Lett.*, 42, doi:10.1002/2015GL064220.